Supporting information

Patterned Macroporous Fe_3C/C Membrane Induced High Ionic Conductivity for Integrated Li-Sulfur Battery Cathodes

Wei Kou, Guohui Chen, Yang Liu, Weixin Guan, Xiangcun Li, Ning Zhang, Gaohong He*

Table S1. Structure parameter comparisons for different membranes

Membrane parameters	$FeCl_3$/PAN membrane	Fe_3C/C membrane	C membrane
Radius (mm)	6	6	6
Thickness (μm)	55	35	42
Mass (mg)	1.895	1.86	2.27
Volume (mm^3)	6.22	3.96	4.75
Apparent density (mg mm^{-3})	1.180	1.948	1.800
Porosity (%)	74.18	75.85	73.45

Table S2. Comparison of electronic resistances of Fe_3C/C and C membranes

	1	2	3	4	5	Average
Fe_3C/C (Ω)	127.4	131.5	109.1	122.7	115.7	121.3
C (kΩ)	1.859	1.772	1.475	1.601	1.679	1.677

Table S3. Comparison of Li-ion diffusion coefficients ($cm^2\ s^{-1}$) in Fe_3C/C and Al cathodes

Samples	D_1 (peak A)	D_2 (peak B)	D_3 (peak C)
Fe_3C/C membrane	3.54×10^{-8}	2.72×10^{-8}	12.89×10^{-8}
Al cathode	1.21×10^{-8}	0.428×10^{-8}	2.13×10^{-8}

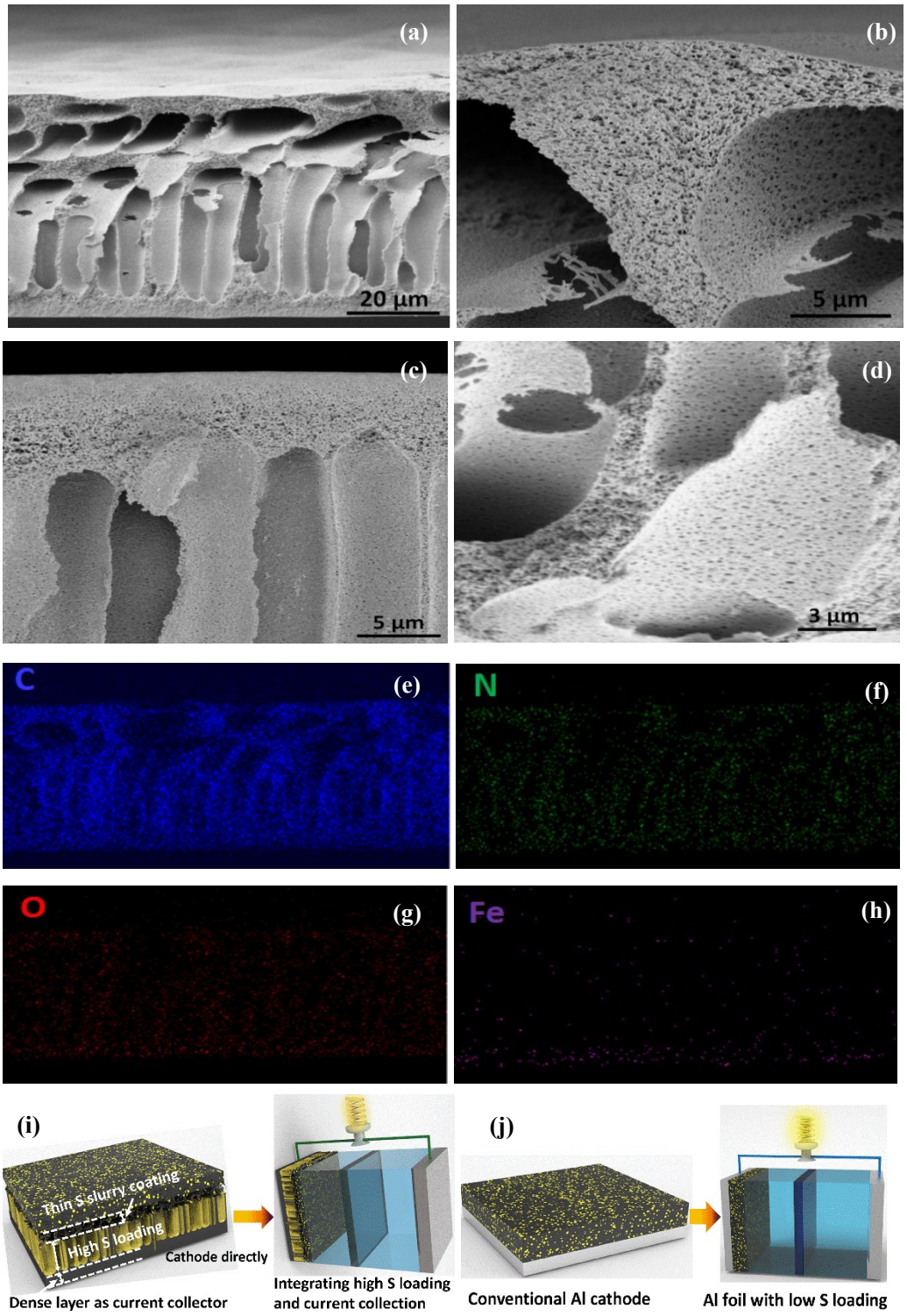

Figure S1. (a) cross-section SEM image of Fe^{3+} doped PAN composite membrane with three-layered structures, (b) top surface with sponge-like pores, (c) bottom layer with dense structure, (d) skeleton of the membrane possesses sponge-like pores, (e-h) uniform distributions of elements C, N, O and Fe throughout the membrane, (i, j) Li-S batteries with Fe_3C/C membrane and Al foil as cathodes respectively.

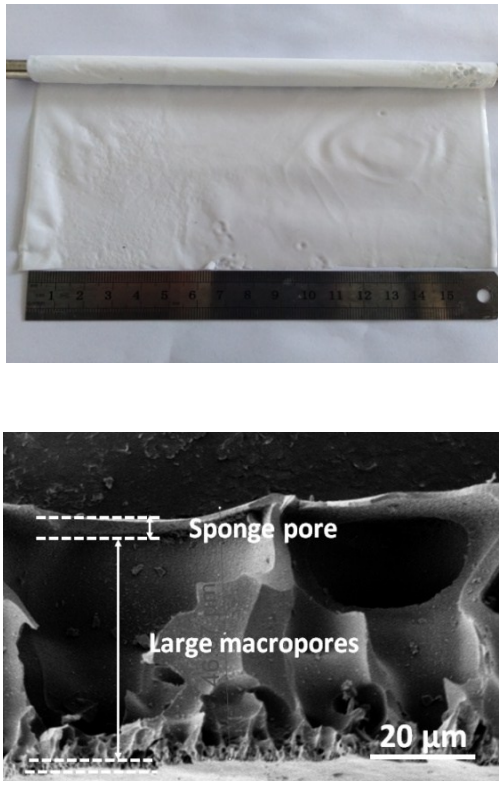

Figure S2. The pure PAN membrane and cross-section SEM image with large macropores

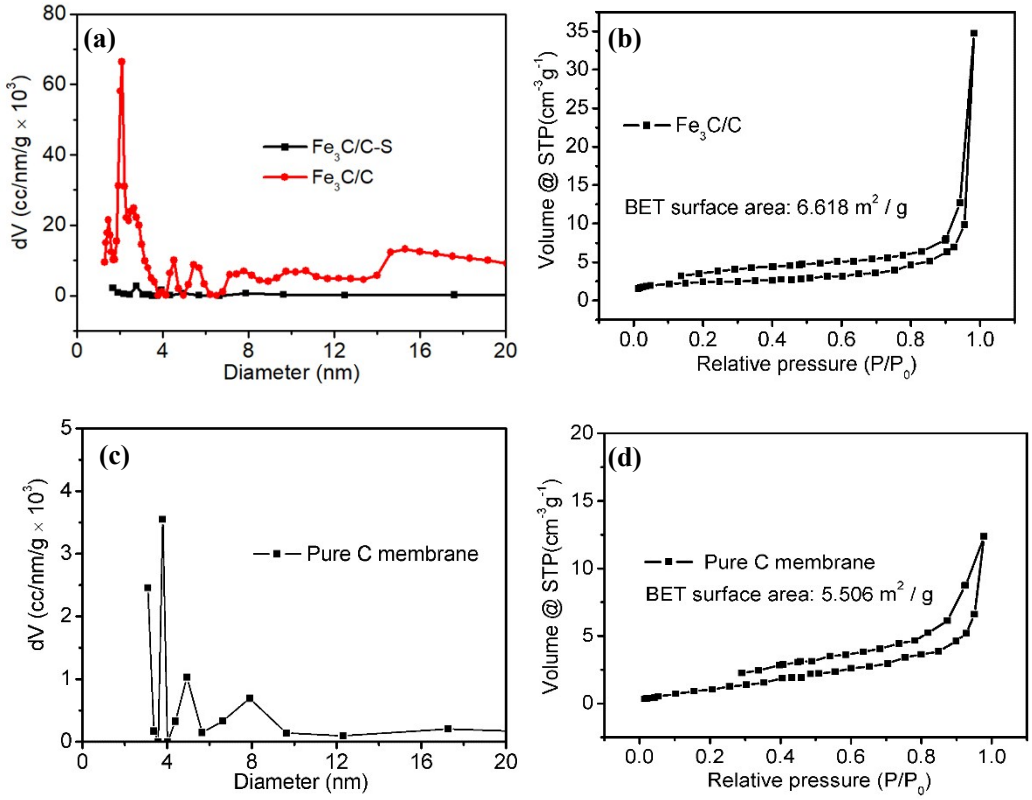

Figure S3. (a) Pore size distribution comparisons between the Fe_3C/C and sulfur-loaded Fe_3C/C membranes reveals that the mesopores in the membrane are successfully filled with S species, (b) N_2 adsorption−desorption isotherms of Fe_3C/C membrane, (c, d) N_2 adsorption−desorption isotherms and the corresponding pore size distribution curves of the pure carbon membrane

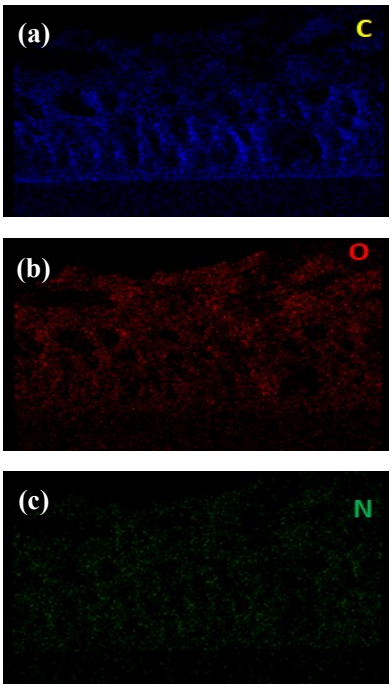

Figure S4. The uniform distributions of C, O and N elements in the membrane

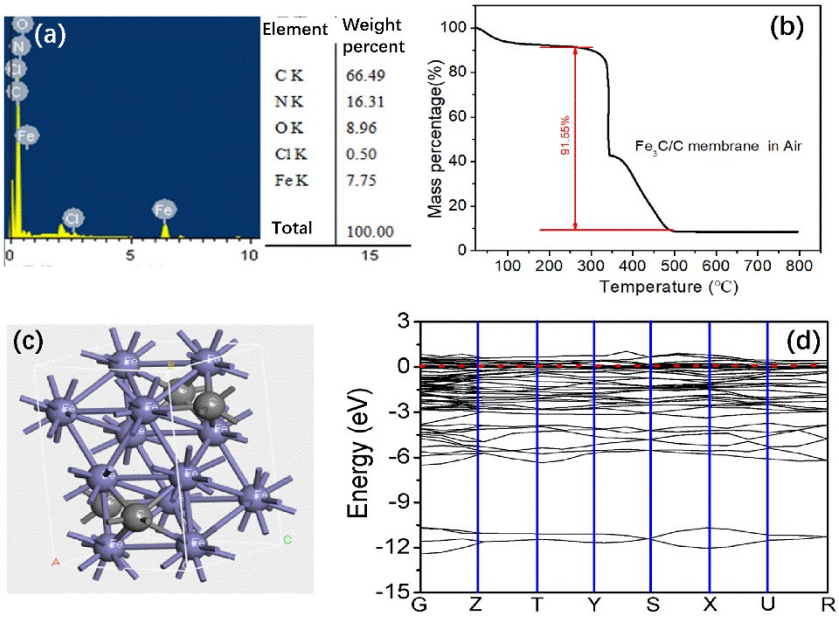

Figure S5. (a) Presence of different elements in Fe_3C/C membrane, (b) mass percentage of Fe_3C in the composite membrane is about 8.5 wt% by TGA analysis, (c, d) crystal structure and calculated electronic band structures of Fe_3C.

Crystal structure and electronic band structures of Fe_3C

As shown in the Figure S5c, d, Fe_3C is an orthorhombic structure with 16 atoms per unit cell, where 4 iron atoms are in "special" positions, 8 iron atoms are in "general" positions, and 4 carbon atoms are in the interstices. Our simulation of band structures exhibits no energy gap near the Fermi level, which demonstrates the metallic nature of Fe_3C with good conductivity.

Lv, Z et.al[1] calculated the electronic properties of Fe_3C based on DFT, confirming that Fe_3C is the unusual mixtures of metallicity, covalence, and ionicity. G. Grimvall and co-workers[2] calculated the ρ of Fe_3C is 47 μΩ cm at 300 K, which is smaller than the value of amorphous carbon materials (~$5*10^4$ μΩ cm), delivering high conductivity.

(1) Lv, Z.; Zhang, F.; Sun, S.; Wang, Z.; Jiang, P.; Zhang, W.; Fu, W., First-principles study on the mechanical, electronic and magnetic properties of Fe_3C. *Computational Materials Science* **2008,** *44*, 690-694.
(2) Häglund, J.; Grimvall, G.; Jarlborg, T., Electronic structure, X-ray photoemission spectra, and transport properties of Fe_3C (cementite). *Physical Review B* **1991,** *44*, 2914.

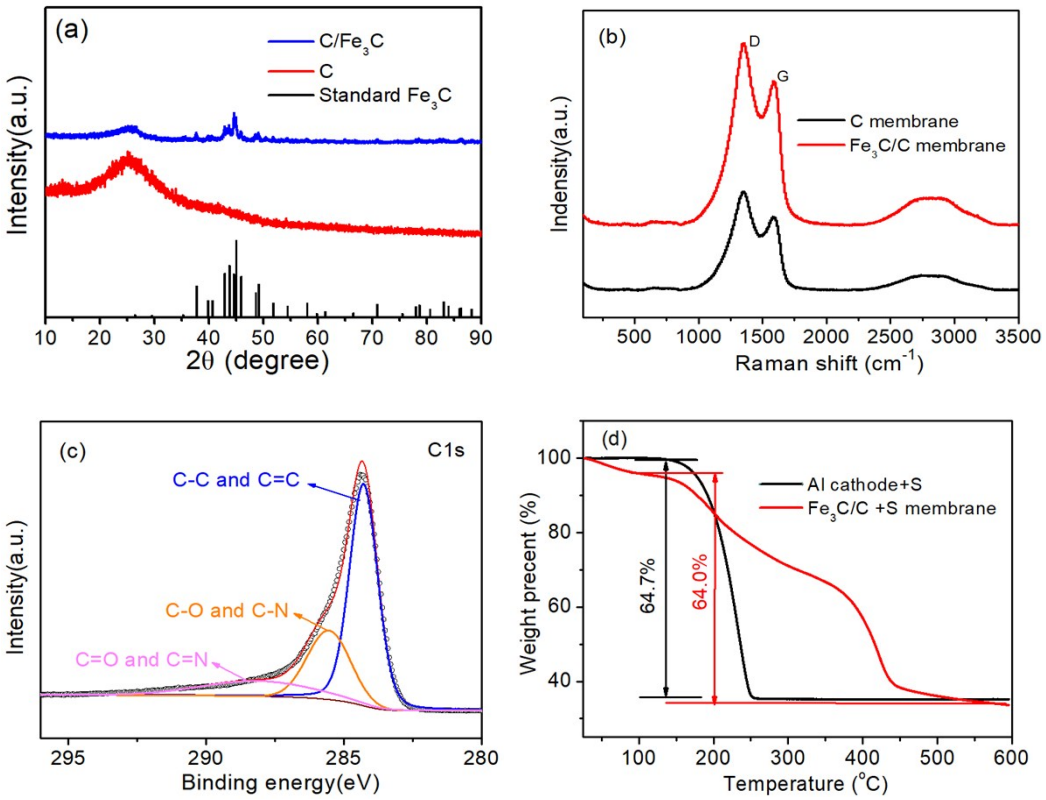

Figure S6. (a) XRD patterns of C and Fe_3C/C composite membranes, (b) Raman and FTIR spectra of the two kinds of membranes, (c) C 1s spectra of the Fe_3C/C membrane, (d) sulfur species in Fe_3C/C membrane shows a higher thermal stability (> 250℃) compared with that in the conventional Al cathode (~250℃) due to the chemical bonding interaction

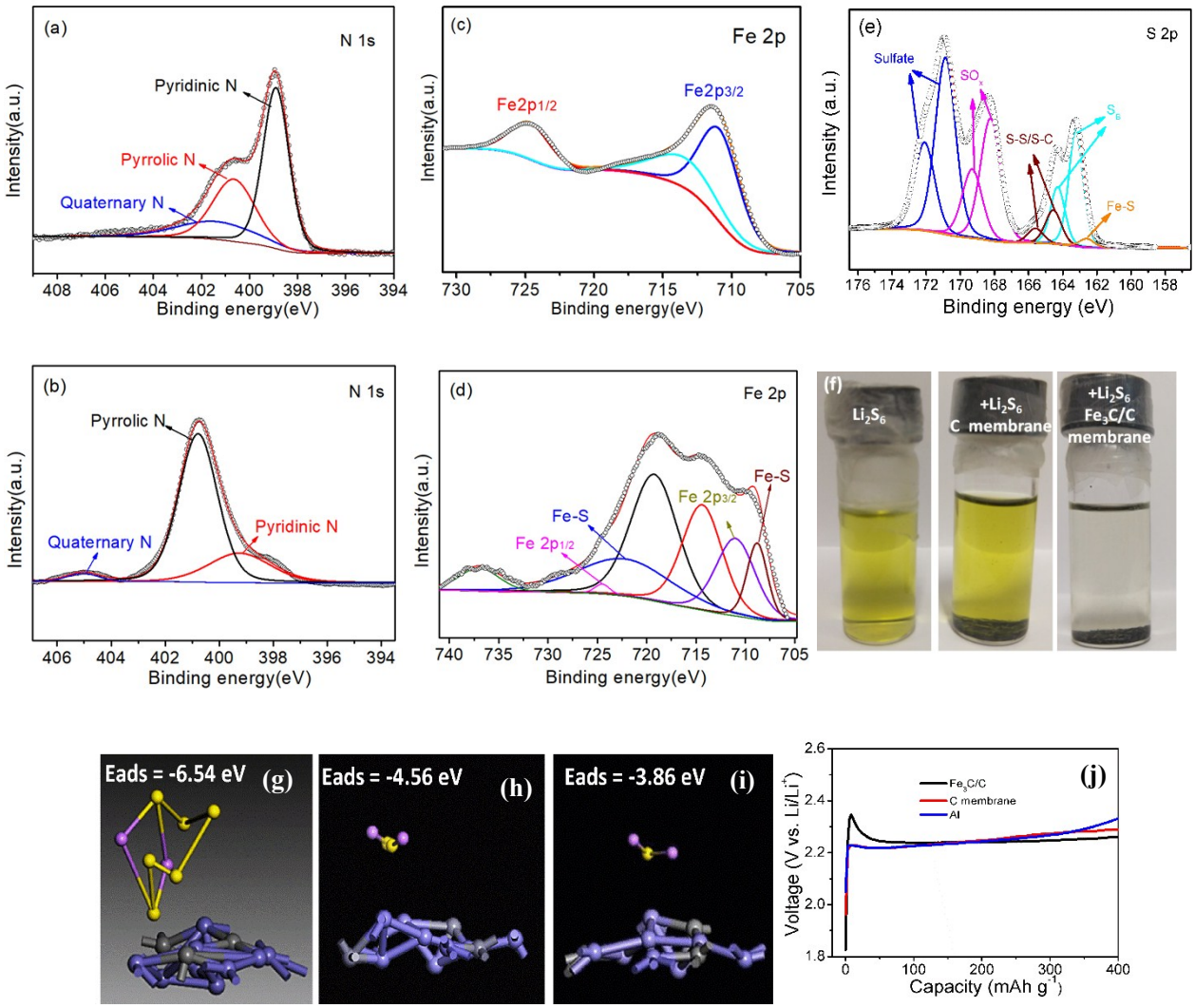

Figure S7. (a, b) the fitted N 1s pattern for Fe_3C/C and sulfur loaded Fe_3C/C membranes at totally discharged state, (c, d) Fe 2p XPS spectra of Fe_3C/C and sulfur loaded Fe_3C/C membranes, (e) S 2p XPS spectrum from the sulfur loaded Fe_3C/C membrane at the state of discharging to 1.7 V, (f) visual adsorption observation of Li_2S_6 on the C and Fe_3C/C membranes, (g-i) DFT simulation of absorption energies between Li_2S_6/Li_2S/Li_2S_2 and the (220) crystal plane of Fe_3C crystal, (j) electrochemical activation on the surface of Fe_3C/C, C membrane and Al foil.

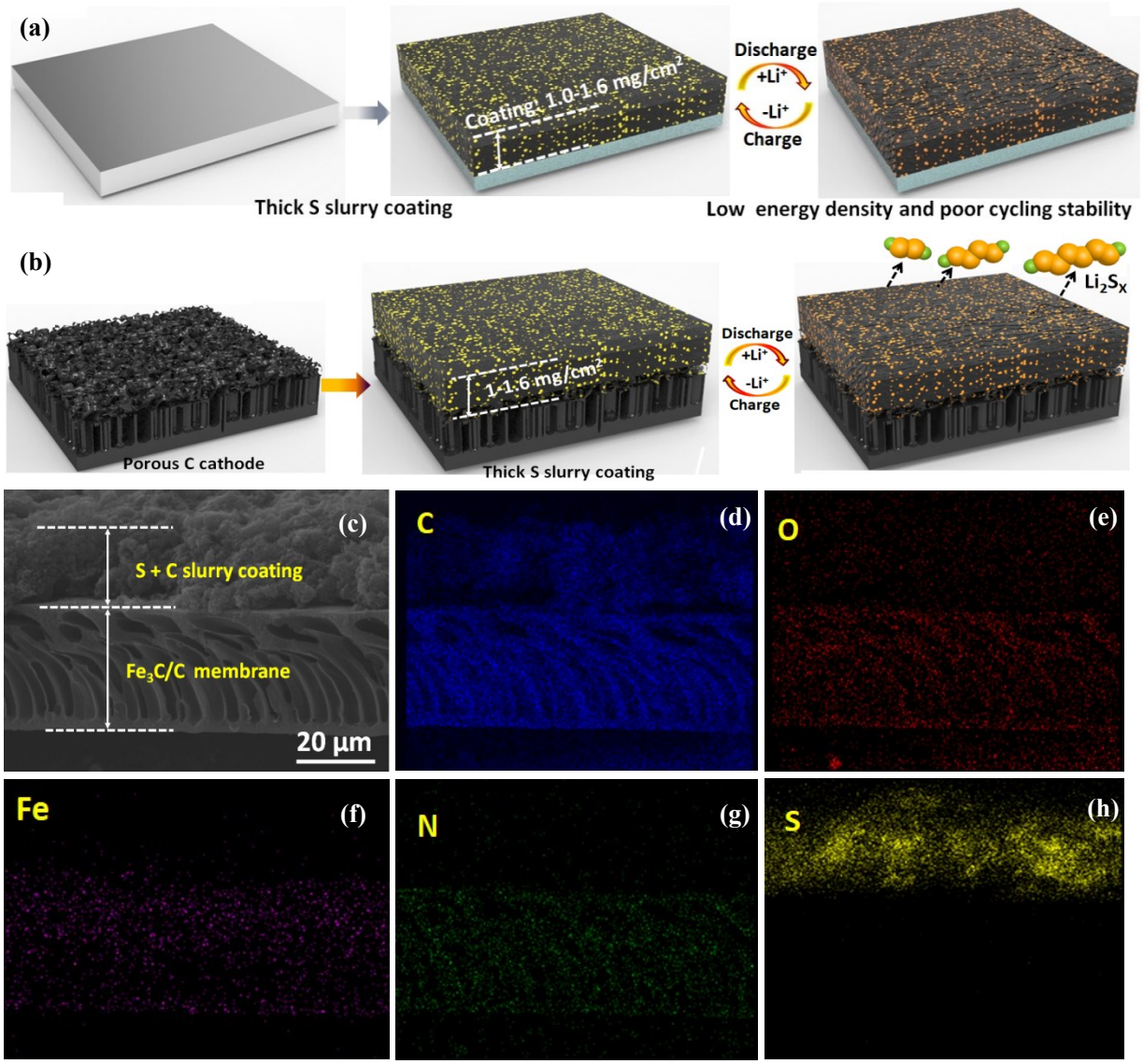

Figure S8. (a) Coating thick S slurry on the conventional Al foil, (b) equivalent thick S slurry were coated on the Fe_3C/C membrane surface, (c-h) SEM image of the S slurry coated Fe_3C/C membrane, and distributions of S and other elements.

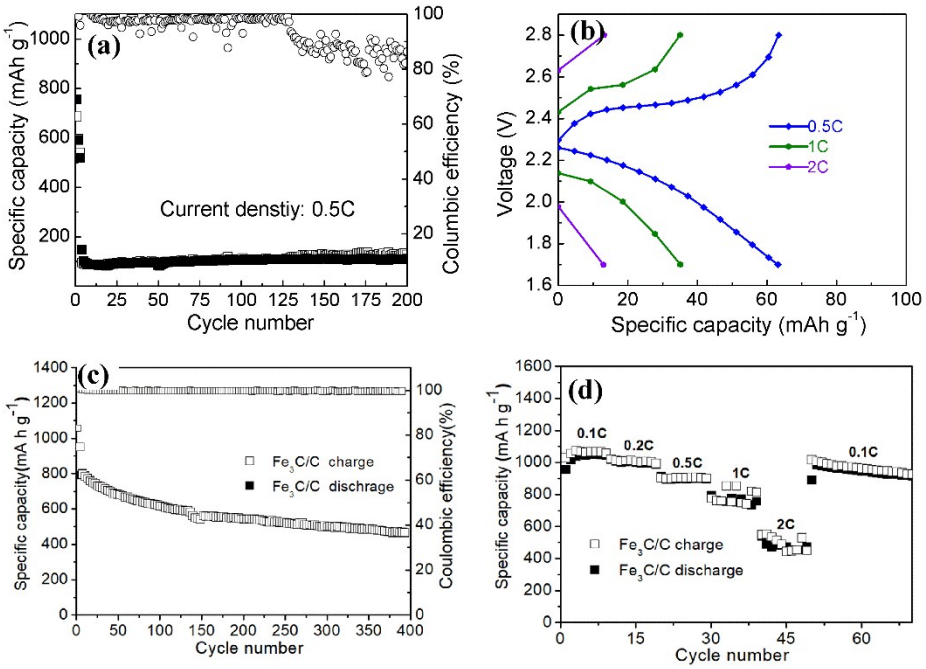

Figure S9. (a, b) Li/Fe_3C cell property in the voltage range of 1.7-2.8 V; (c, d) the thick S slurry coated membrane cathodes show inferior rate capacities and cycling stability (0.5C) due to the high Li^+ transfer resistance and the weak interaction between the membrane and LiPSs

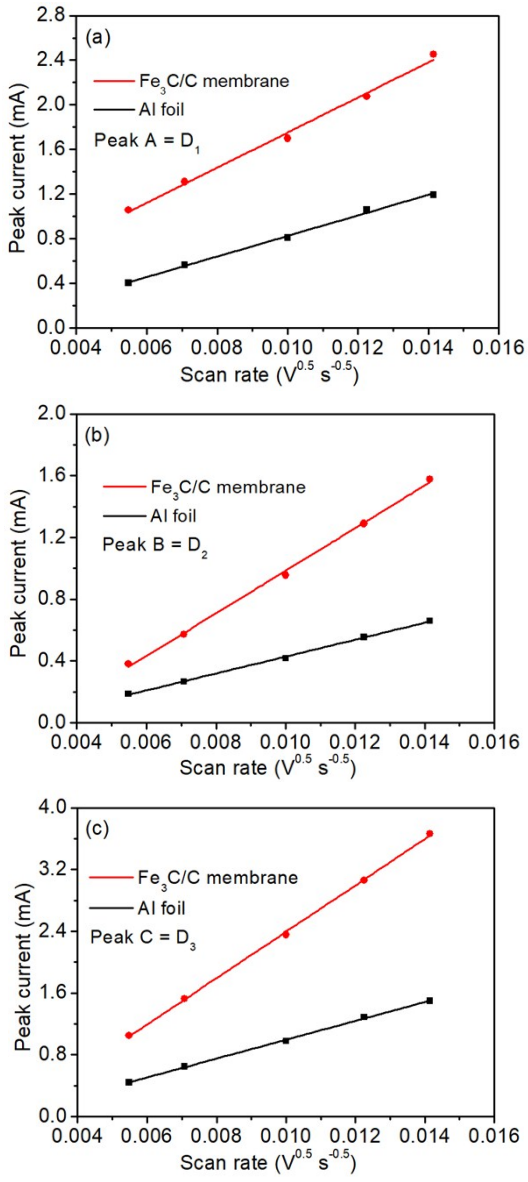

Figure S10. Lithium-ion diffusion coefficients were calculated based on the Randles-Sevcik equation

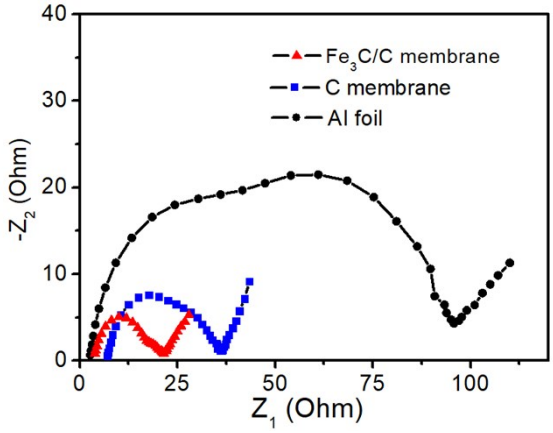

Figure S 11. Electrochemical impedance spectra of Fe_3C/C membrane, C membrane and Al foil cathodes

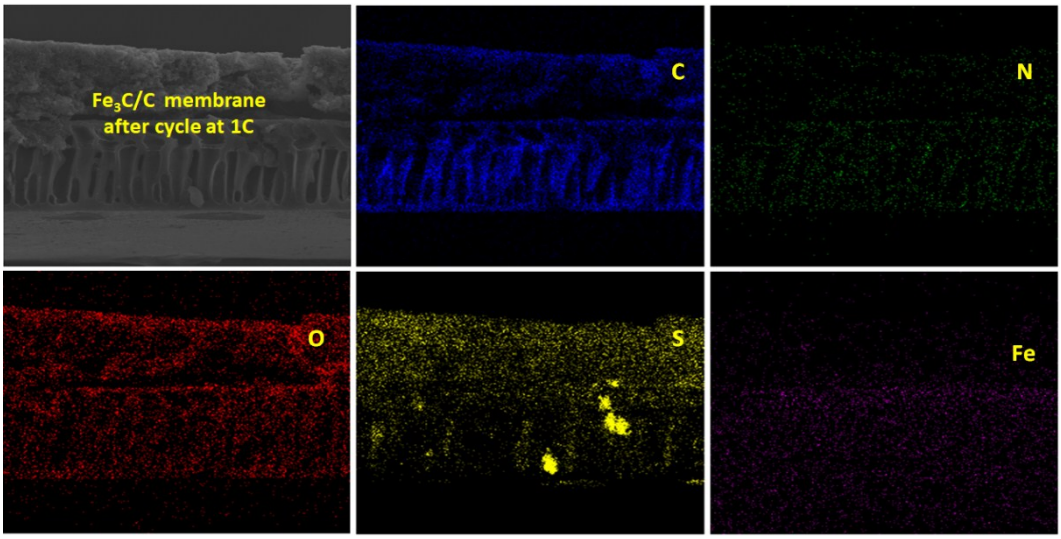

Figure 12. The distributions of different elements after long-term cycle in the Fe_3C/C membrane